

TUMORS INVADING PARAPHARYNGEAL SPACE: REFINED IMAGING DIAGNOSIS

Zhuang Qixin 庄奇新 Cheng Yingsheng 程英升 Yang Shixun 杨世坝
Shang kezhong 尚克中 Yan Xinhua* 严信华

*Department of Radiology, and *Otolaryngology, Shanghai Sixth Hospital, Shanghai 200233*

Objective: To investigate imaging findings of tumors invading parapharyngeal space. **Methods:** Magnetic resonance imaging (MRI) computerized tomography (CT), magnetic resonance angiography (MRA) and digital subtraction angiography (DSA) findings of 19 patients with tumors infiltrating parapharyngeal space by surgery and pathology were analysed, including four branchial cleft cysts, three jugular glomus tumors, four carotid body tumors, three neurilemmomas and five carcinomas of nasopharynx involving parapharyngeal space. Fifteen patients underwent MRI scanning nine patients had CT scanning, three patients MRA and five patients DSA. **Results:** MRI provided clinically useful informations about the size, shape, extent and site of the parapharyngeal space tumors, and also their effects on adjacent structures. The main MRI features of paraganglioma presented as many low signal tortuous and creeping vessels in the tumor. The main CT features of jugular glomus tumor revealed as jugular foramen enlargement with bone destruction. Tumor vessels were clearly displayed by MRA and DSA. **Conclusion:** MRI was superior to CT in the diagnosis of tumors invading parapharyngeal space. The location and nature of the lesions could be diagnosed accurately by MRI combined with CT or DSA.

Key words: Pharyngeal neoplasms, Magnetic resonance imaging, Computerized tomography, X-ray computer, Angiography.

The parapharyngeal space (PPS) is a difficult

region to evaluate clinically. The PPS lies beneath the mandible, the sternocleidomastoid muscle, and the parotid gland. Routine X-ray examinations are often indistinguishable. Great strides have been made in the imaging diagnosis of lesions involving the PPS.¹ In this study we analyzed the imaging features in nineteen patients with tumors infiltrating the PPS proved by surgery and pathology since 1991.

MATERIALS AND METHODS

Since 1991, fifteen MR and nine CT scan, five DSA and three MRA examinations in nineteen patients with tumors including four branchial cleft cysts, three jugular glomus tumors, four carotid body tumors, three neurilemmomas and five carcinomas of nasopharynx by surgically proved PPS masses were reviewed. There were 12 male and 7 female patients aged 19-55 years.

MR images were performed on 1.0T SMT-100 imager (Schimadzu, Japan) and obtained with multi-section, spin-echo (SE) proton-density-weighted and T2-weighted and SE T1-weighted techniques. The imaging technical factor varied; for T1-weighted images repetition times (TRs) of 500 msec and echo times (TEs) of 18 msec were used, and for proton-density-weighted and T2-weighted images TRs of 2000 msec with first echo TEs of 20 msec and second-echo TEs of 90 msec were used. All MR images had a section thickness of 5 mm. The acquisition matrix was 256×256. Transverse, coronal and sagittal scans were obtained. CT scanning was performed on 600S unit

Accepted July 17, 1997

(Toshiba, Japan), with 5-mm-thick contiguous section obtained in the axial plane. Scanning factors of 120 KV and 300 mA were used. The acquisition matrix was 512×512. DSA images were performed on DAR-1200C angiographic apparatus. The contiguous exposition times of 15 msec in carotid arteriography were used. MRA used method of “time flight”.

RESULTS

The masses invading PPS in 19 patients lay deep in the soft-tissue spaces of cervical part. CT scanning with 3 patients with branchial cleft cyst was used. The CT appearance of the lesions were fluid areas of low attenuation with an ovoid and sharply outlined mass in medial part of cervical muscle, PPS was disoblited. On contrast-enhanced computerized tomography (CECT), carotid sheath was displaced internally (Figure 1). Branchial cleft cyst in 1 patient was well circumscribed and homogeneously low in signal intensity on T1-weighted images (T1WIs) and homogeneously high in signal intensity on T2-weighted images (T2WIs). MRI and CT scans in 3 patients with jugular glomus tumors were used. MRI appearances of the tumors were well circumscribed (Figure 2, 3). On T1WIs and T2WIs, this combination of foci of signal void within a high signal mass has been termed the “salt and pepper” appearance. The main CT features of jugular glomus tumors revealed as jugular foramen enlargement with bone destruction (Figure 4). MRI and MRA or DSA examinations in 4 patients with carotid body tumors were used. The MRI features

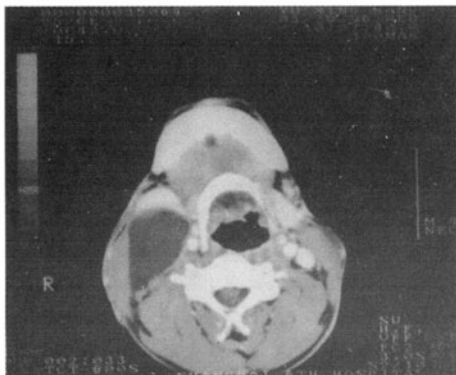


Fig. 1. Right branchial cleft cyst. On CECT, the lesion showed fluid area of low attenuation with ovoid and sharply outlined mass. PPS was disoblited, carotid sheath was displaced internally.

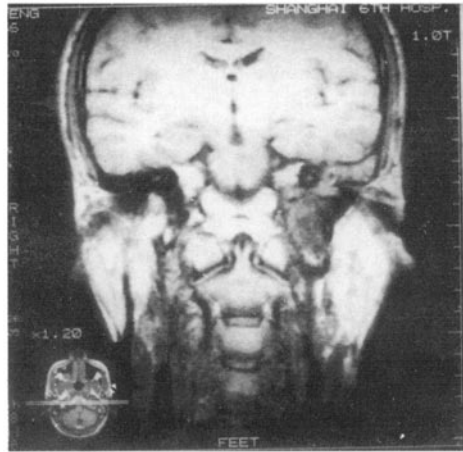


Fig. 2. and Fig. 3. Left jugular glomus tumor. On coronal and transverse T1WIs of MRI, the tumor was well circumscribed. There were small creeping vessels in the tumor (arrow).

presented as many low signal tortuous and creeping vessels in the tumor (Figure 5). Tumor vessels were clearly displayed by MRA and DSA (Figure 6, 7). DSA and MRI features showed enlarged and braced bifurcation between internal carotid artery and external carotid artery by mass (Figure 5, 7). MRI features in 3 patients with neurilemmomas were smoothly outlined, and the internal and external carotid arteries and internal jugular veins were displaced (Figure 8). DSA examination in 2 patients with neurilemoma was used. Tumor vascularity in neurilemoma was less than that in carotid body tumor (Figure 9). 2 MR images and 5 CT scans in 5 patients with nasopharynx carcinomas involving PPS were used. The CT appearance of the

lesions was a soft-tissue mass. Choanae and accessory nasal sinuses were invaded anteriorly, and medial and lateral pterygoid muscles invaded by mass. The lesions were hypointense on T1WIs and hyperintense on T2WIs (Figure 10).



Fig. 4. with Fig. 2. The same case. On CT, left jugular foramen enlargement with bone destruction (arrow).

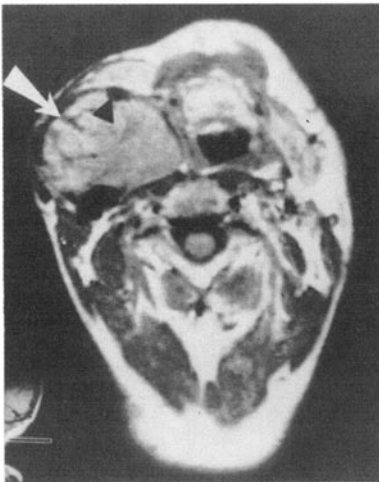


Fig. 5. Right carotid body tumor. On transverse T1WIs of MRI, there were many tortuous and creeping vessels in the tumor (straight arrow) with low signal intensity. The bifurcate angle between internal carotid artery and external carotid artery was enlarged and braced by mass (arrow).

DISCUSSION

The PPS extends from the level of the oropharynx to the skull base and is bordered anterolaterally by the pterygoid muscles and posterolaterally by the parotid gland. Medially it is bordered in the

oropharynx by the pharyngeal constrictors and tonsillar pillars and in the nasopharynx by the palatal muscles (Figure 11). The styloglossus muscle, where it inserts into the tongue, closes the inferior extent of the PPS posteriorly.² In addition to fat, the PPS contains branches of the third division of cranial nerve V, the ascending pharyngeal artery, internal maxillary artery branches, and pharyngeal veins.

The PPS has a high signal intensity on T1WIs and PD images and decreases to an intermediate signal on T2WIs. It has a low attenuation on CT scan.

Primary PPS neoplasms are rare. They account for less than 0.5% of head and neck neoplasms. Most PPS neoplasms are benign. The common PPS tumors are pleomorphic adenoma, lymphoma, paraganglioma, neurogenic tumors.^{3,4}

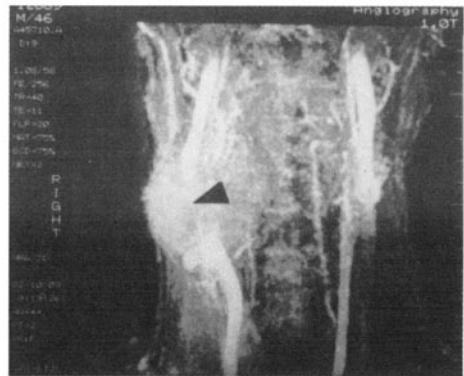


Fig. 6. The same case with Fig. 5. On coronal image of MRA, tumor vessels were clearly displayed (arrow).

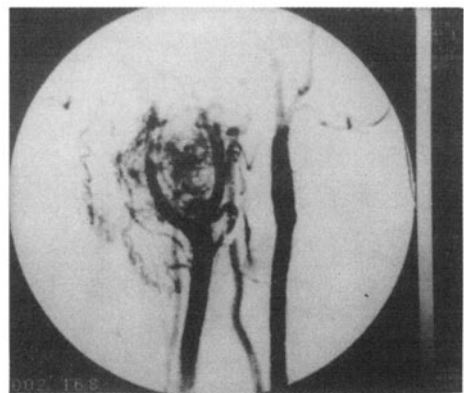


Fig. 7. The same case with Fig. 5. On DSA, the bifurcate angle between internal carotid artery and external carotid artery was enlarged and braced by mass, tumor vessels were clearly displayed (arrow).



Fig. 8. Left neurilemoma. On transverse PDWIs of MRI, the internal carotid artery, external carotid artery and internal jugular vein were displaced externally by tumor (arrow).

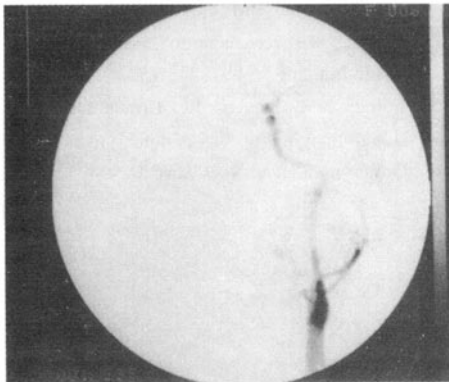


Fig. 9. The same case with Fig. 8. On DSA, tumor vessels were less than that in carotid body tumor.

Brachial cleft cysts lie in PPS before styloid process. It is homogeneously low in signal intensity on T1WIs and homogeneously high in signal intensity on T2WIS.

Paragangliomas are hypervascular tumors that arise from chemoreceptor cells at multiple sites in the head and neck region. The glomus jugular originates in the jugular bulb, frequently erodes the skull base around the jugular foramen, and may extend intracranially or inferiorly into the carotid space. Carotid body tumors arise at the carotid bifurcation and usually are lower in the neck, but may extend upward

into the PPS. Paragangliomas are intermediate in signal intensity on T1WIs and moderate to high intensity on T2WIs. These lesions tend to displace the internal carotid artery anteriorly prior to MRI, the distinction of these masses requires either dynamic CT scanning or angiography. In our study, MRI in 4 patients with carotid body tumors presented low in signal intensity, and were tortuous and creeping vessels in the tumors.⁵ Other MRI features were enlarged and braced in bifurcate angle between internal carotid artery and external carotid artery by mass.

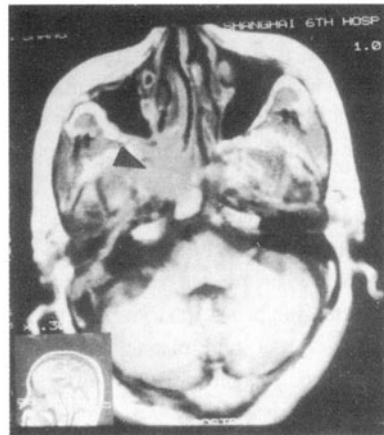


Fig. 10. Right nasopharynx carcinoma. On transverse T1WIs of MRI, the choana, accessory nasal sinuses and PPS were invaded by nasopharynx carcinoma (arrow).

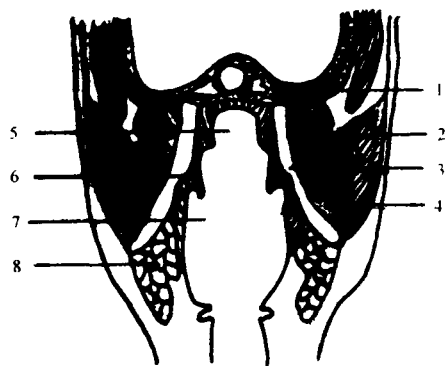


Fig. 11. Schematic drawing of parapharyngeal space. 1. Skull base; 2. Pterygoid muscle; 3. Parapharyngeal space; 4. Mandible; 5. Nasopharynx; 6. Pharyngeal constrictor; 7. Oropharynx; 8. Mandibular gland

Neurogenic tumors of the carotid space include neurilemoma and neurofibromas. Most arise from the

vagus nerve, but they also may originate in the sympathetic chain or in cranial nerves.⁶ On T1WIs, small neuromas usually are homogeneous and intermediate in signal intensity. Larger lesions, although predominantly intermediate signal, often contain foci of high (hemorrhage) and/or low (cystic degeneration or necrosis) signal intensities. On T2WIs, schwannomas are intermediate to high in signal intensity, and the interspersed areas of hemorrhage, necrosis, and cystic degeneration usually are higher in signal than the main portion of the tumor.⁷ In our study, MRI in 3 patients with neurilemoma are low in signal intensity, neurilemoma displaces the internal carotid artery and external carotid artery and internal jugular vein.

Malignancies of PPS or adjacent related spaces may spread by direct extension, along muscles and tissue planes, via lymphatics or neurovascular bundles. Tumor may extend inferiorly into the floor of the mouth and upper neck or superiorly to involve the skull base. In our study, PPS was invaded in 5 patients with nasopharynx carcinoma. MRI may display the invading extension of nasopharynx carcinoma.

Having direct multiplanar imaging capability, MRI allows the diagnostician to offer his clinical colleagues a more accurate assessment of the total extent of disease and a better map of the spatial relationship of tumors to crucial vessels.⁸ MRI were

superior to CT in diagnosis of tumors invading parapharyngeal space. The location and nature of the lesions could be diagnosed accurately by MRI combined with CT or DSA.

REFERENCES

1. Som PM, Curtin HD. Lesions of the parapharyngeal space: role of MR imaging. *Otolaryngol Clin North Am* 1995; 28:515.
2. 李果珍, 戴建平, 王仪生. 临床 CT 诊断学. 北京: 中国科学技术出版社. 1994; p364.
3. Hughes KV, Olsen KD, McCaffrey TV. Parapharyngeal space neoplasms. *Head Neck* 1995; 17: 124.
4. Stanley RE. Parapharyngeal space tumors. *Ann Acad Med Singapore* 1991; 20:589.
5. 陈星荣, 沈天真, 段承祥, 等. 全身 CT 和 MRI. 上海医科大学出版社. 1994; p208.
6. 王弘士, 杨天锡, 顾雅佳. 颈动脉间隙肿瘤的 CT 诊断. *中华放射学杂志* 1994; 28:677.
7. Tom BM, Rao VM, Guglielmo F. Imaging of parapharyngeal space: anatomy and pathology. *Crit Rev Diagn Imaging* 1991; 31:315.
8. Lofchy NM, Steyens JK, Brown DH. Three-dimensional imaging of the parapharyngeal space. *Arch Otolaryngol Head Neck Surg* 1994; 120:333.